

Summary of Dissipation Measurements from the Absolute Velocity Profiler (AVP) during the Hawaiian Ocean Mixing Experiment, R/V Wecoma, Oct. 9-30, 2000

Jonathan Nash
Tom Sanford, Craig Lee and Eric Kunze
Applied Physics Laboratory, University of Washington.
— Draft Cruise Report —

March 13, 2001

1. Introduction

The principal objective of our AVP profiling during HOME was to determine the structure, variability, energy flux and dissipation associated with the internal wave field. This was accomplished by gathering an ensemble of vertical profiles (usually 10; five upward and 5 downward) of the motionally-induced electric fields at a given station over a period of 14 hours.

In total, 78 vertical profile pairs were obtained at 14 station locations, two of which were repeated to determine temporal variability. Profiles of turbulent velocity shear were obtained using shear probes on each downward profile from near the surface to within 1 m of the bottom (nominally 3000 m) at a speed of 1 m/s.

2. Signal Processing

2.1. Instrumentation Details

Dissipation measurements were made on AVP using two shear probes (VG1 and VG2; VG= “velocity gradient”) sampled at 416.7 Hz. These were located approximately 6” from the centerline, and were angled so that the oncoming flow is along the shear probe’s axis as the probe traces a slightly helical path down the water column while AVP rotates at approximately 0.2 revolutions per second. The shear probes were oriented to measure the vertical gradient of the radial component of the horizontal velocity (with respect to AVP’s centerline).

2.2. Sources of Noise

The minimum TKE dissipation rate that can be measured by AVP is a function of 1) the proximity of the shear probes to a turbulent wake generated by AVP’s drop weights; 2) the mechanical vibration of the AVP body/velocity-gradient sensor can; and 3) whether or not AVP’s acoustic doppler was pinging.

2.2.1. Wake of Drop-weights:

The turbulent wakes from two drop weights (located 0.5 m and 2.0 m ahead of the sensors) may be sampled by the shear probes. During the HOME cruise, VG1 was almost continuously measuring the wake of the weights instead of oceanic turbulence. Five meter averages of the dissipation rate ϵ (denoted ϵ_5) from VG1 were seldom less than $10^{-6} \text{m}^2 \text{s}^{-3}$. More commonly these estimates were $10^{-5} - 10^{-4} \text{m}^2 \text{s}^{-3}$. The rms shear amplitude from VG1 was modulated at a 5-6 second period, leading us to hypothesize that the probe oscillates through different parts of the wake at the same frequency as the rotation rate of AVP.

A simple calculation indicates that the measured dissipation from VG1 is consistent with that of the wake. If the weights have an O(1) drag coefficient, then the integrated specific momentum imparted to the flow is

$$M_o = u_o A_o = 1 \text{ m/s} \cdot \pi (.025 \text{m})^2 \quad (1)$$

$$M_o = 2 \times 10^{-3} \text{ m}^3/\text{s} \quad (2)$$

This is the initial integrated momentum. Assuming a 10% spreading rate (ie., $\ell = 0.10(z - z_o)$ where $(z - z_o)$

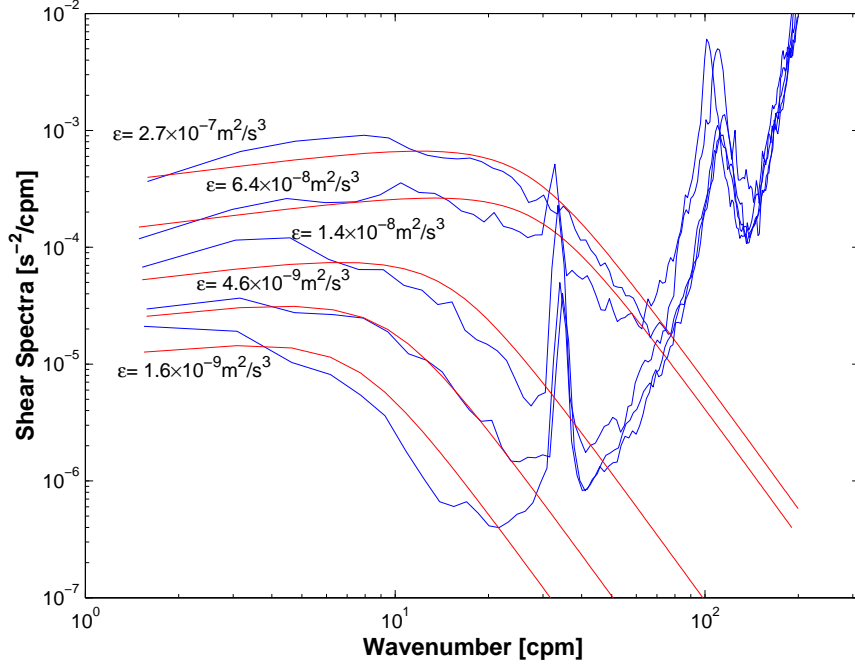


Figure 1: Spectra of velocity shear (u_z) for five patches of turbulence (blue) and the corresponding Nasmyth empirical form (red). In order of increasing dissipations: i) AVP764, 2100m–2150m; ii) AVP764, 3020m–3040m; iii) AVP764, 370m–385m; iv) AVP764, 45m–75m; v) AVP768, 2730–2780m.

is the distance from the virtual origin, assumed to be at the weight), then the wake 2 m downstream has an area $A_2 = 0.12\text{m}^2$. Equating the initial momentum with the final, $M_2 = M_o$, we find that

$$u_2 = M_o/A_2 \quad (3)$$

$$u_2 = 0.016 \text{ m/s} \quad (4)$$

Based on the large eddies ($u_2 = .016 \text{ m/s}$, $\ell = 0.20 \text{ m}$) we find the dissipation rate in the wake to be

$$\epsilon = \frac{u^3}{\ell} = 2 \times 10^{-5} \text{ m}^2\text{s}^{-3} \quad (5)$$

This is consistent with the magnitude of ϵ measured by VG2.

Fortunately, the slight asymmetry of the instrument which placed VG1 continuously in the wake was responsible for keeping the second shear probe, VG2, outside of it and it sampled undisturbed, oceanic turbulence. VG2 recorded 5m average dissipations below $5 \times 10^{-9}\text{m}^2\text{s}^{-3}$ for continuous depth intervals exceeding 500 m, which we consider to be representative of the AVP's noise floor in its current configuration. While the noise level appears

to be relatively constant over the duration of any particular drop, the minimum detectable ϵ_s may vary by a factor of 10 between drops. It is believed that the difference in noise level is a function of the configuration of the particular pair of drop weights which hang below the sensors.

2.2.2. Mechanical Vibration:

There are three components to the mechanical vibration of AVP. Figure 1 shows shear spectra for the range of dissipations that AVP's 2nd shear probe (VG2) was capable of measuring throughout the duration of the cruise. VG1, for reasons described below, produced no useful shear measurements.

There is a vibrational peak in the shear spectrum at approximately 30-35 cpm, which roughly corresponds to the 33 Hz pump frequency of the pumped Seabird CTD (2000 rpm). There is also noise near 100 Hz, which is quite high for a mechanical vibration; perhaps it is electrical or is induced by the sampling (it is close to $F_{Nyquist}/2$). All calculations of ϵ_s were made from wavenumbers below 30 cpm, and hence do not include noise from either of these narrow-band signals.

There is a broadband noise floor between 1-10 cpm, which has a similar signature to that of turbulence. It could be the edge of the wake or the low-frequency vibration of many different components of the instrument. Regardless of what its source, it is very constant in time, and the estimates of the instrument-induced dissipation are robustly characterized in a statistical sense.

2.2.3. Acoustic Doppler

The doppler was only turned on during a small fraction of the profiles. There are two modes of operation: 1) searching for bottom (5 seconds between pings) and 2) tracking the bottom (2 Hz ping rate). In both modes, pinging introduces one-sided (positive) single spikes into the shear signal. It is not known whether the contamination is acoustical or electrical.

In the first mode of operation, estimates of ϵ_5 are only slightly above that of the base noise level. In the second mode, the ping rate is ten times more frequent, and the effect on ϵ_5 is unacceptable. Fortunately, the exact times of pinging are recorded, and it is hoped that the ping contamination can be substantially reduced from the shear record. Only a couple profiles were affected by the second mode of acoustical contamination.

2.3. Characterization of the Noise

As a result of the variability of the noise floor, the pdf of $\epsilon_5(z)$ was calculated for each profile for depths below 500 dbar. For most profiles, the shape of this pdf is dominated by the noise, because much of the oceanic dissipation in this region is less than $5 \times 10^{-9} \text{m}^2 \text{s}^{-3}$.

While the median dissipation in the deep ocean may be below $5 \times 10^{-9} \text{m}^2 \text{s}^{-3}$, the mean of the dissipation is dominated by the largest events, which are often much larger than $10^{-8} \text{m}^2 \text{s}^{-3}$, and can be much larger. In order not to bias averages of ϵ high by the instrument's relatively high noise level, much effort has been made to characterize the noise and discard all estimates that are at or below the noise threshold of the instrument. kplu.org

The noise threshold of each AVP profile was calculated by determining the mean μ and standard deviations σ of $\log_{10} \epsilon_5$ for depths greater than 500 m for each drop (see Figure 2 for an example). In most cases, the distribution contains an approximately log-normal region which I have assumed represents the instrument noise, and a tail which extends to higher dissipations, which I assume is

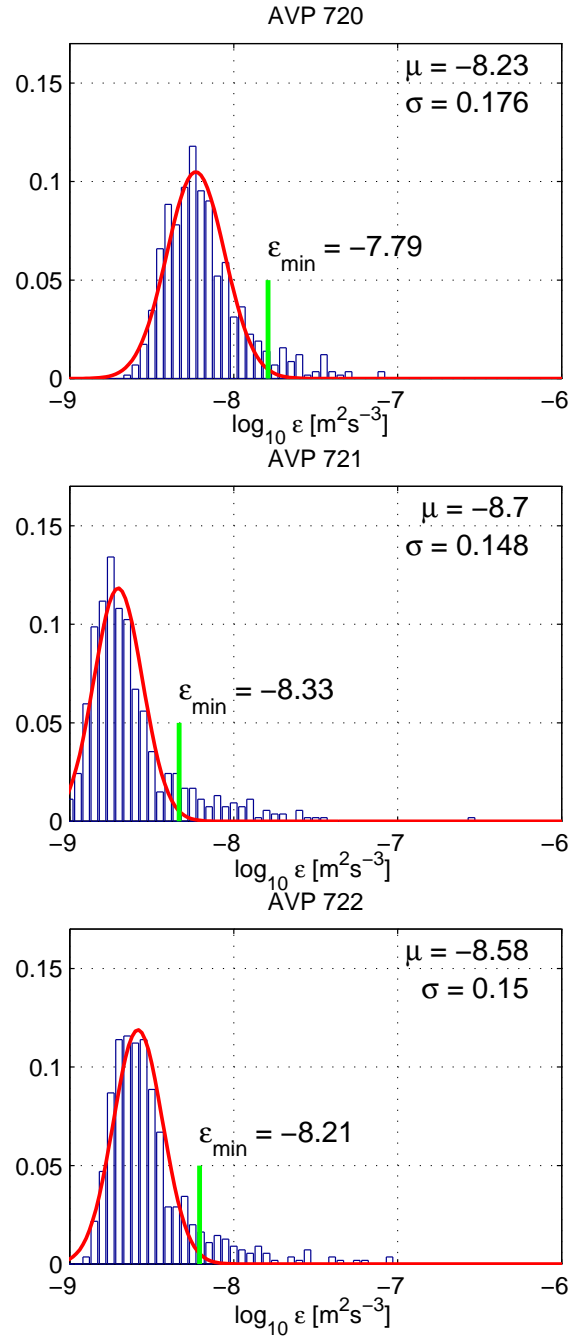


Figure 2: Distributions of 5m-binned dissipation (ϵ_5) for depths greater than 500 m for three consecutive AVP profiles indicate the variability of the noise floor. The red curve represents a log-normal distribution with mean μ and standard deviation σ as indicated. The green vertical bars represent $\epsilon_{noise} = \mu + 2.5\sigma$, an estimate of the minimum observable dissipation for that profile.

signal. I calculate μ and σ , remove all estimates exceeding $\mu + \alpha_o\sigma$, and repeat this procedure until the mean and standard deviation of the remaining points is stable; α_o is a parameter which I have chosen to be $\alpha_o = 2.5$ and simply represents the number of standard deviations above the mean of $\log_{10} \epsilon_5$ which I consider to be noise. The minimum detectable dissipation is set to:

$$\epsilon_{noise} = \mu + 2.5\sigma \quad (6)$$

The example in Figure 2 indicates that the noise floor has a variable mean but relatively constant standard deviation. For most of the profiles, the above method produced a satisfactory estimate of ϵ_{noise} . However, for a few of the profiles where substantial energetic turbulence was observed deep in the water column, this automated procedure failed, and it was necessary to select a low-signal depth range by hand. This was done by searching a filtered time series (high passed at 1 m, low passed at 20 Hz) for regions with low rms shear, and applying the above characterization to that region alone.

2.4. Quality-controlled ϵ and K_ρ

To be confident that estimates of ensemble-averaged dissipation at a given station $\epsilon = \langle \epsilon_5(z) \rangle_{z,t}$ represent ocean turbulence and not instrument noise, I have performed the averaging of ϵ_5 in two ways.

- **ϵ_{max}**

First, I average all of the estimates of ϵ_5 in a given depth bin together, regardless of whether the estimates are above or below the instrument's noise floor. This represents the maximum possible dissipation, ϵ_{max} , and provides an estimate of the true mean ϵ_{true} only in regions where $\epsilon_{true} > \epsilon_{noise}$

- **ϵ_{min}**

Second, I estimate the minimum measurable dissipation (ϵ_{noise}) for each profile using equation 6. All estimates of ϵ_5 which fall below this value are set to zero. Averages of ϵ_5 now represent a lower bound, ϵ_{min} on the true dissipation. In strong turbulence, this asymptotes to ϵ_{max} . At turbulence levels near ϵ_{noise} , however, ϵ_{min} may be significantly less than ϵ_{noise} .

The assumption is that the mean of the true dissipation (ϵ_{true}) is dominated by a few turbulent events which are above ϵ_{noise} and that most of the remaining events are much less than ϵ_{noise} and do not substantially contribute to $\langle \epsilon_{true} \rangle$. Hence this estimate ϵ_{min} should only slightly bias the average of ϵ_{true} low, and in general, should be a

better estimate of the mean when the dissipation rate is low.

A comparison of the depth-averaged dissipation using either ϵ_{min} or ϵ_{max} illustrates that the possible error introduced by the noise floor of AVP is minimal. The average ϵ_{min} at any of our 16 station occupations was never less than half that of ϵ_{max} , and the mean of $\epsilon_{min}/\epsilon_{max}$ was 0.7. Thus, using either method (ϵ_{min} or ϵ_{max}) to estimate the bulk dissipation should not change the estimate of total dissipation by more than 30%.

3. Interpretation of Observations

Included at the end of this report are individual profiles of the 5 m dissipation (ϵ_5), organized in groups by station. Also plotted are station-averaged dissipations (ϵ) and eddy-diffusivities $K_\rho = 0.2\epsilon/N^2$, binned into 100 m vertical intervals, and estimated using the two different methods of averaging. These will be referred to as ϵ_{min} and ϵ_{max} ; see section 2.4. for details. I consider ϵ_{min} as the best estimate of the true dissipation with instrument noise removed.

Weak Mid-depth Turbulence

The station-average profiles indicate that turbulence is weak ($\epsilon \sim 10^{-9} \text{m}^2 \text{s}^{-3}$) in the central part of the water column ($1000 \text{ m} < z < 2500 \text{ m}$) at most of the stations.

Bottom Boundary Layer

Intensified turbulence was observed in the bottom 100–300 m of the water column at most stations. 50–200 m thick regions of increased turbulence intensity ($\epsilon \sim 10^{-8} - 10^{-7} \text{m}^2 \text{s}^{-3}$) were observed in this region, most notably at stations 5, 7, 9, 10, 12, 14.

Energetic Near-Surface Dissipation

The upper 1000 m accounted for most of the depth-integrated dissipation at all stations. The dissipation rate increased from its mid-depth value of $10^{-9} \text{m}^2 \text{s}^{-3}$ at $\sim 1000 \text{ m}$ to approximately $10^{-7} - 10^{-6} \text{m}^2 \text{s}^{-3}$ in the upper 100 m depth bin.

The intensified dissipation in the upper part of the water column is consistent with our estimates of internal wave energy flux, which is also largest in the upper part of the water column. Figure 3 shows that there is a strong

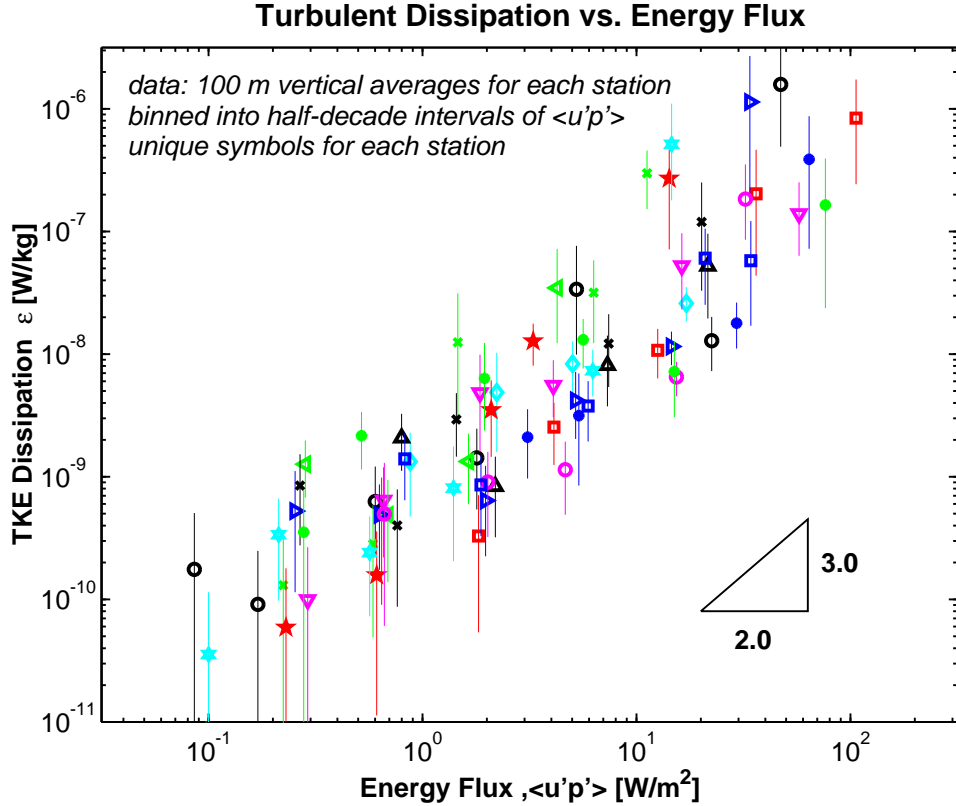


Figure 3: Relationship between average TKE dissipation rate and the specific IW energy flux at all AVP stations during HOME. Estimates of the internal wave energy flux are calculated from $\langle u'p' \rangle_{100}$ averaged over a tidal cycle and are binned into 100m intervals. Dissipation rate (ϵ_{100}) also represents 100 m station averages. In this plot, the energy flux has been binned into half-decade ranges; each data point represents the average dissipation rate ($\langle \epsilon_{100} \rangle$) corresponding to a particular range of energy flux. Error bars represent the 95% bootstrap confidence limits on the mean.

correlation between average TKE dissipation rate and the specific IW energy flux at all AVP stations. The depth-integrated dissipation and flux reveal a similar trend, as shown in Figure 4. A chart of the HOME survey region showing our measured internal wave energy fluxes is included as Figure 5 for reference.

4. Conclusions

The noise level of AVP was $\epsilon_{noise} \sim 5 \times 10^{-9}$ which was low enough to detect the turbulent events at all depths throughout the water column.

Our observations suggest that most of the dissipation in the HOME region is associated with strong turbulence in the upper 1000 m of the water column, which is consistent with the fact that most of the internal wave energy flux is also located there. Intensified dissipation was also

observed near the bottom, but does not contribute substantially to the depth-integrated dissipation.

Our comparisons of the total dissipation rate to internal wave energy flux suggests that these are related, and has allowed us to estimate an e-folding decay scale of the internal wave field due to local turbulent processes, which is approximately 1000 km.

5. Station Summary Plots

The average dissipation and eddy diffusivity for each station occupation is plotted in Figures 6 – 20.

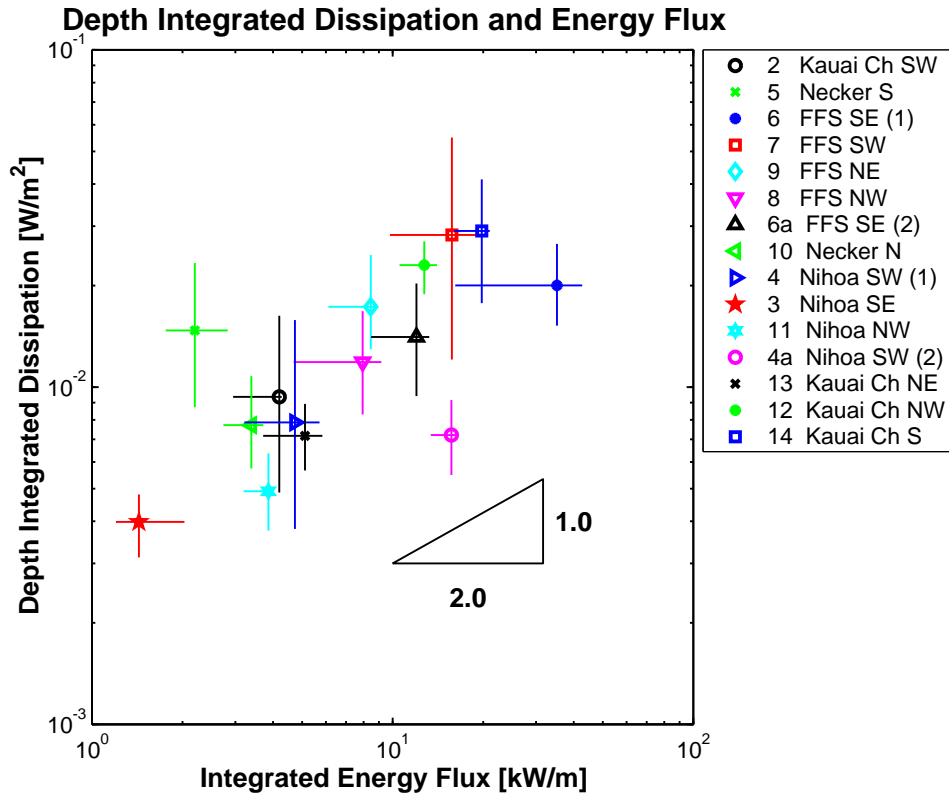


Figure 4: Relationship between the depth-integrated TKE dissipation rate and the total IW energy flux. Error bars represent 95% bootstrap confidence limits on the mean.

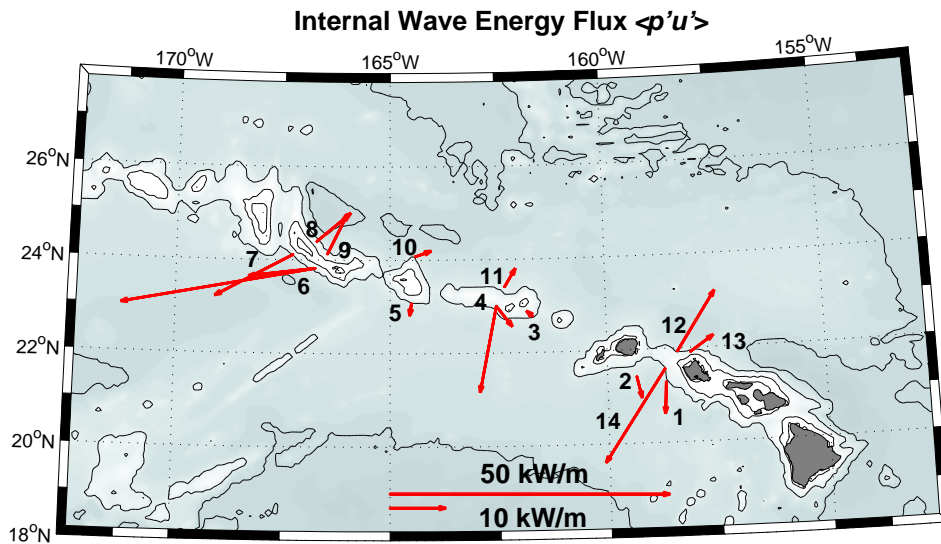


Figure 5: Chart of the Hawaiian Island region showing the depth-integrated internal wave energy flux inferred from station averages of $\langle p'u' \rangle$ as measured by AVP. Numbers are the station numbers from 1 to 14.

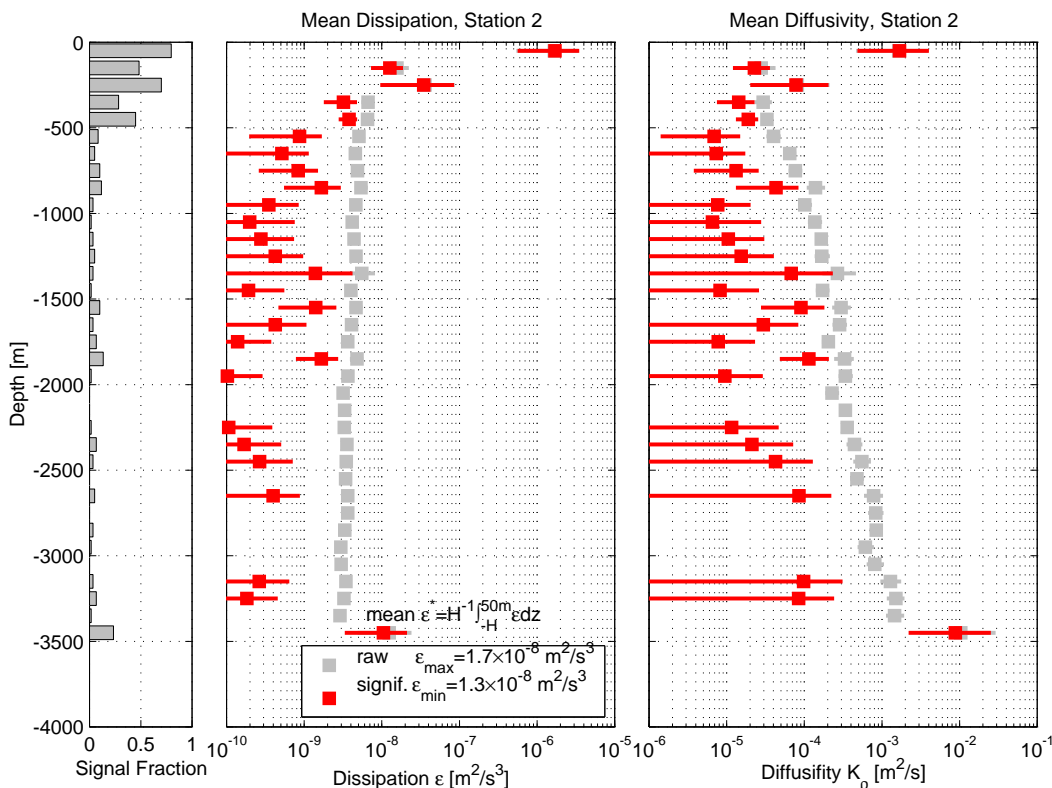


Figure 6: Mean dissipation and diffusivity for Station 2. Data have been binned into 100 m intervals and averaged over 4-5 profiles spanning ~ 12 –14 hours. Grey symbols denote quantities computed from the raw ϵ without accounting for instrument noise. Red symbols represent averages in which all 5 m dissipations (ϵ_s) less than the instrument noise ϵ_{noise} are set to zero prior to averaging. The histogram to the left indicates the fraction of ϵ_s estimates within each 100 m bin which exceed ϵ_{noise} . Error bars represent 95% bootstrap confidence limits on the mean. Values of the depth-averaged dissipation rate are indicated in the inset.

6. Appendixes

6.1. Appendix A: Instrument Log for ϵ .

Shear probes were installed on AVP starting on drop 708. VG1 (shear probe no. 270) was noisy, but VG2 (no. 260) was quiet, with a noise floor of $\sim (2 - 5) \times 10^{-9} \text{m}^2 \text{s}^{-1}$.

On drop 710, we replaced VG1 with no. 256, and it was still noisy. On drop 711, VG1 was replaced again by no. 255, but this did not help.

For drop 713, we shortened the drop weight line from 94" to 80", believing that the noise was caused by the wake from the weight. It is not clear that this has helped the situation at all.

A deck check was performed (file oct13a), and on deck, both probes behave similarly (VG1 might be somewhat noisier than VG2).

We concluded that VG1 was in the wake and VG2 was

outside of it, as noted earlier in this report. We continued to profile in the same configuration as AVP713 until drop 769. At this point we made a change because the last five drops (765–769) had a significantly larger ϵ_{noise} than we would have wished. Tom suggested that we move the weight release line slightly closer to VG1 in an effort to increase the distance between the wake of the drop weights and the VG2 sensor. For drops AVP770 and later, we wrapped the weight release line one turn around the spider (one of the three ropes which connect the release line to the cage) closest to VG1. The distance the line was moved from the center axis was approximately 3/4". This had a significant effect on the performance of the shear probes, lowering ϵ_{noise} by a factor of 10 from its high level during 765–769.

On drop 777 (our second-to-last drop), shear probe VG2 developed a problem and did not produce quality

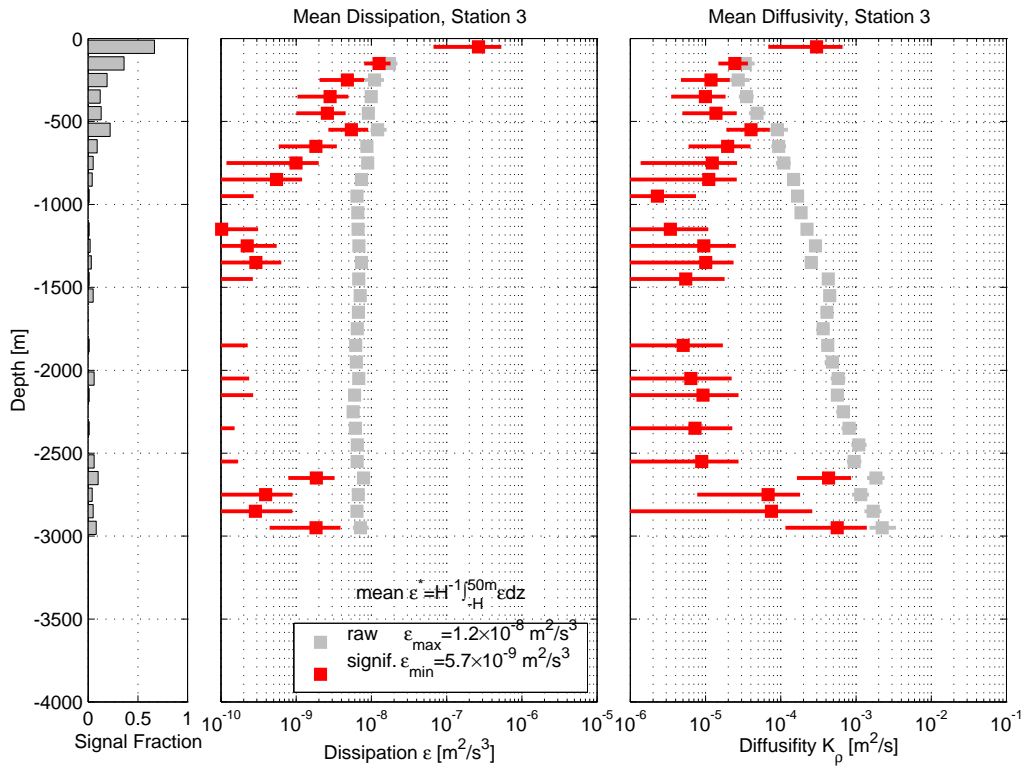


Figure 7: Dissipation and diffusivity for Station 3

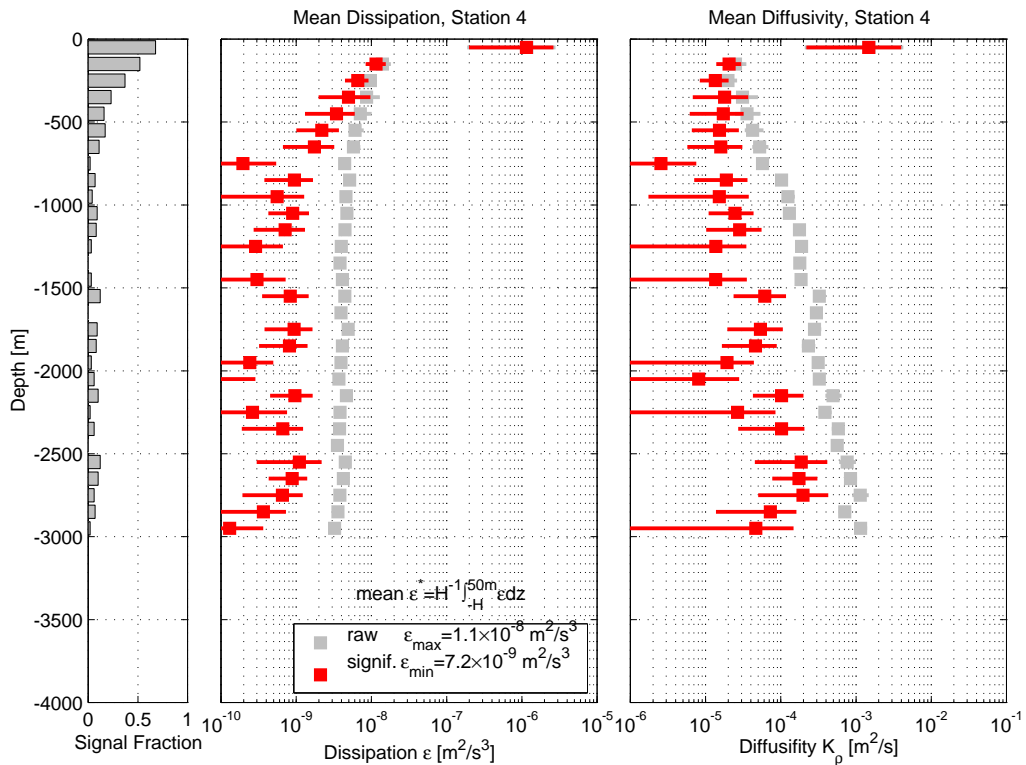


Figure 8: Dissipation and diffusivity for Station 4

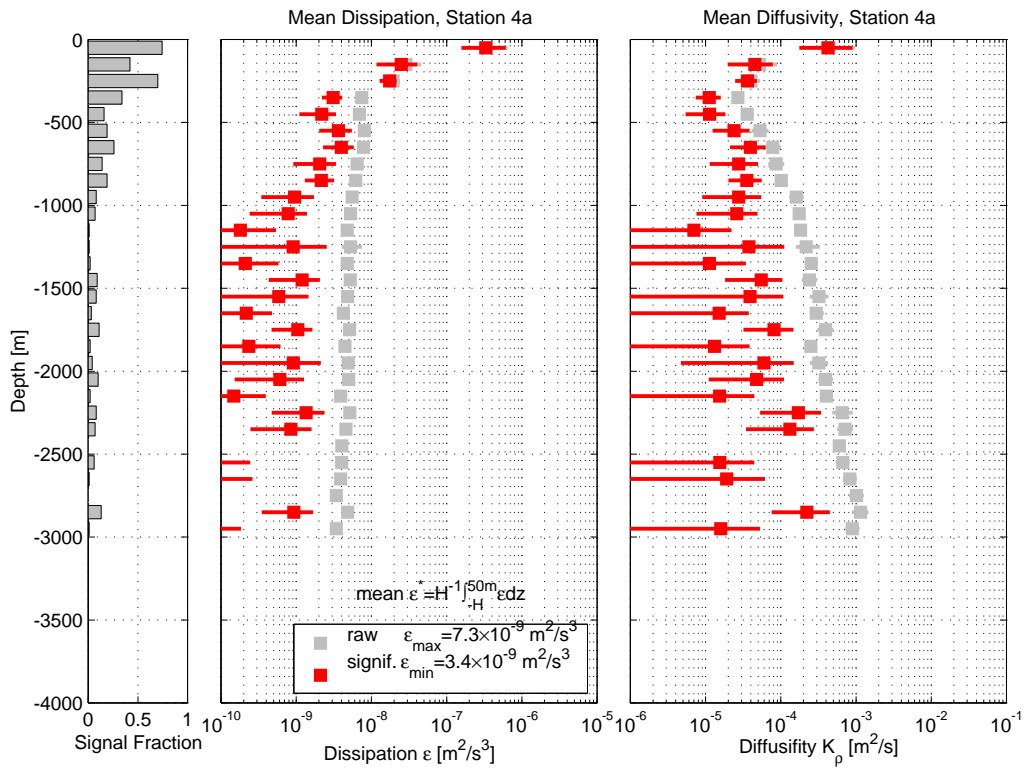


Figure 9: Dissipation and diffusivity for Station 4a

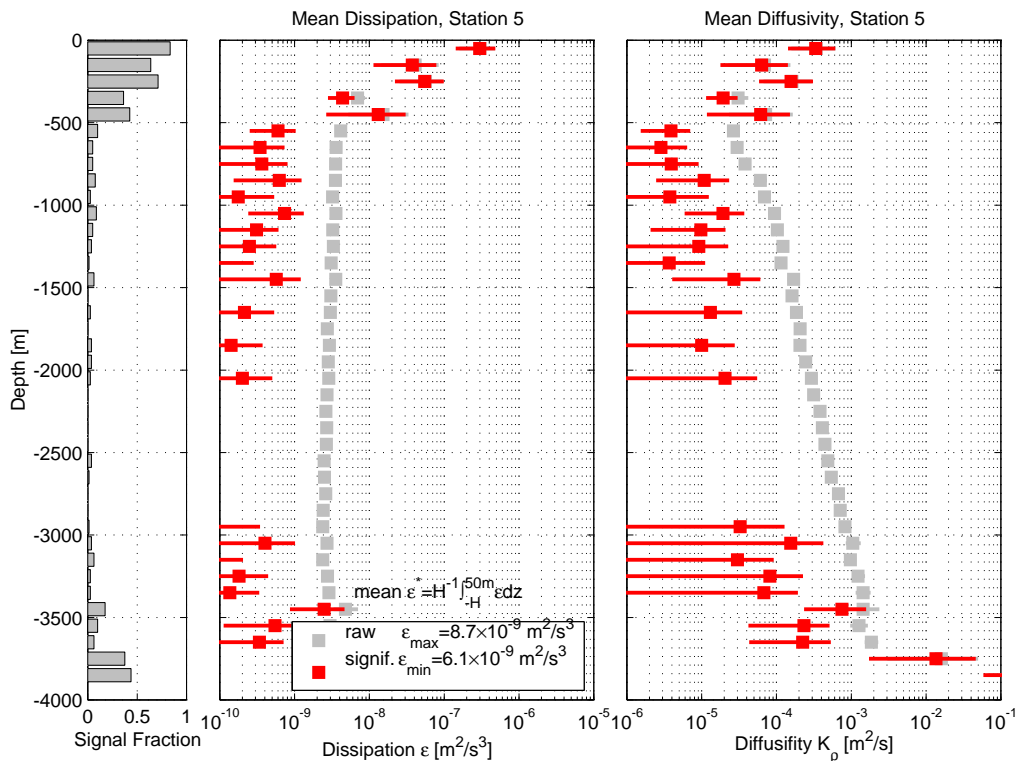


Figure 10: Dissipation and diffusivity for Station 5

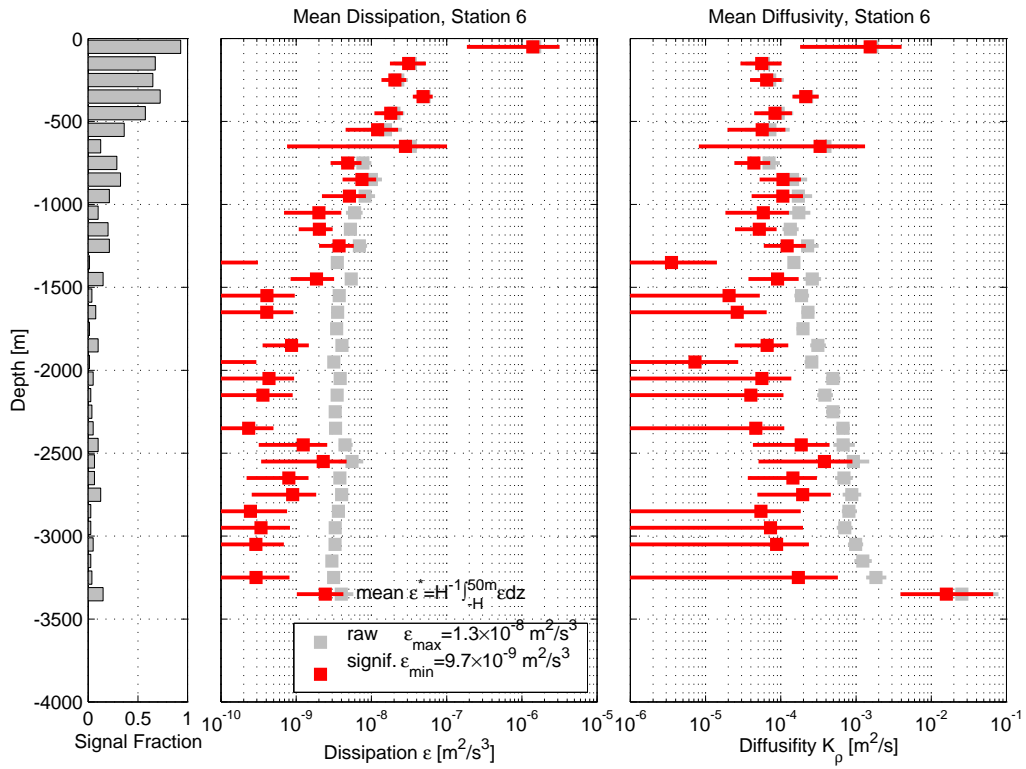


Figure 11: Dissipation and diffusivity for Station 6

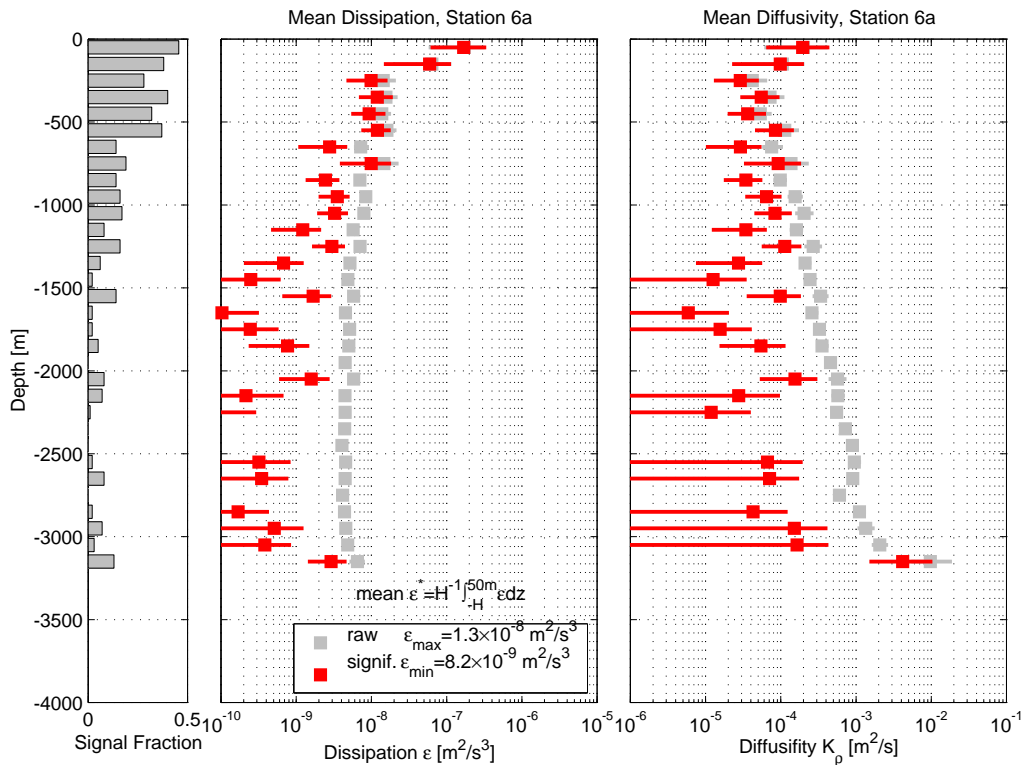


Figure 12: Dissipation and diffusivity for Station 6a

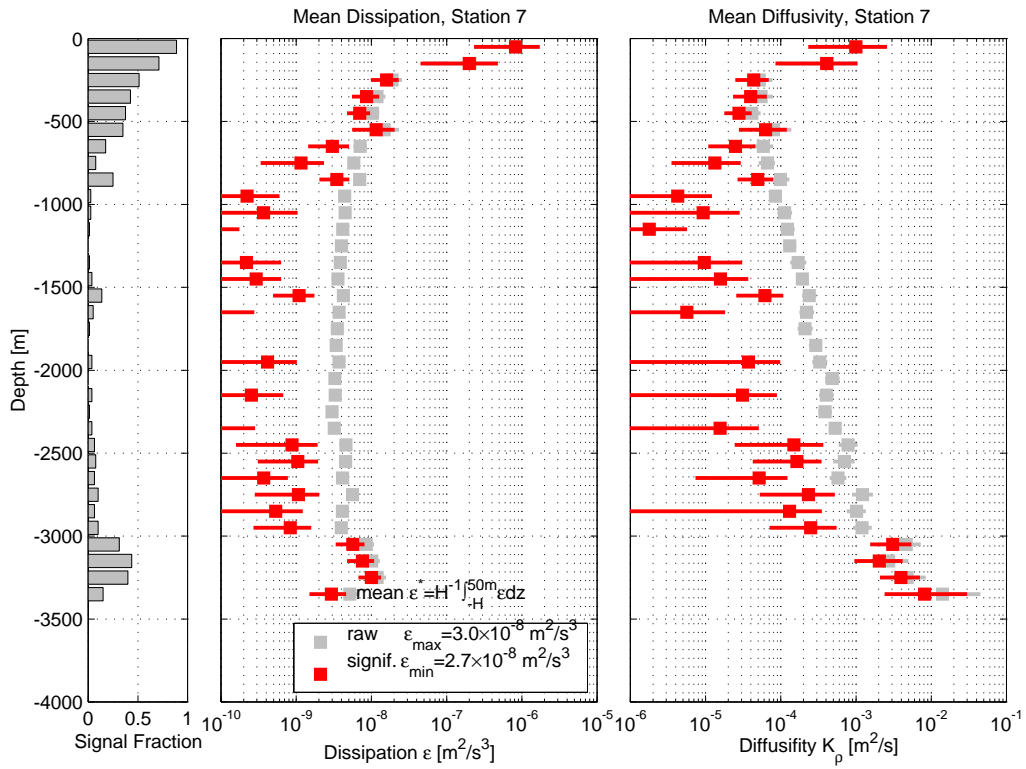


Figure 13: Dissipation and diffusivity for Station 7

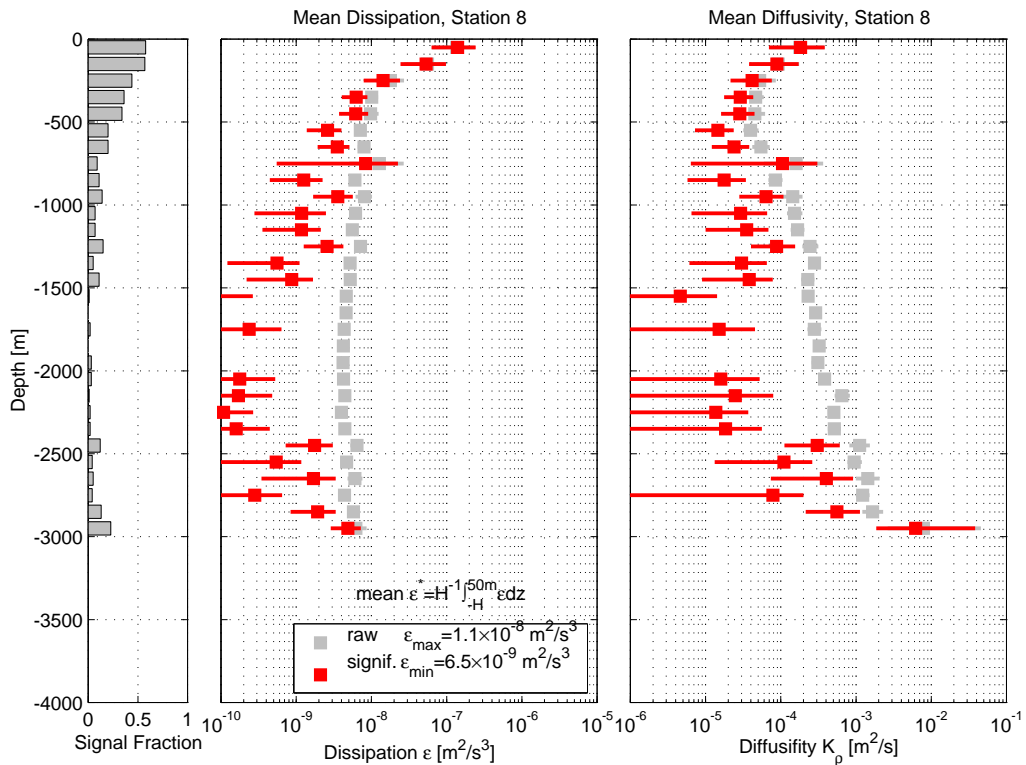


Figure 14: Dissipation and diffusivity for Station 8

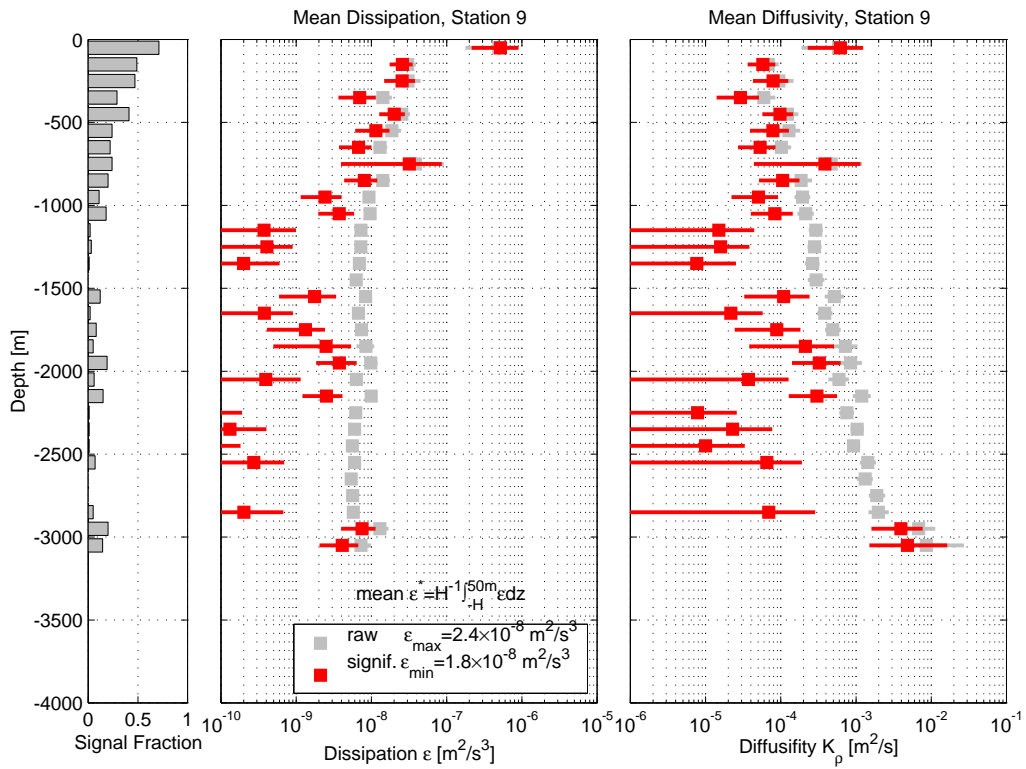


Figure 15: Dissipation and diffusivity for Station 9

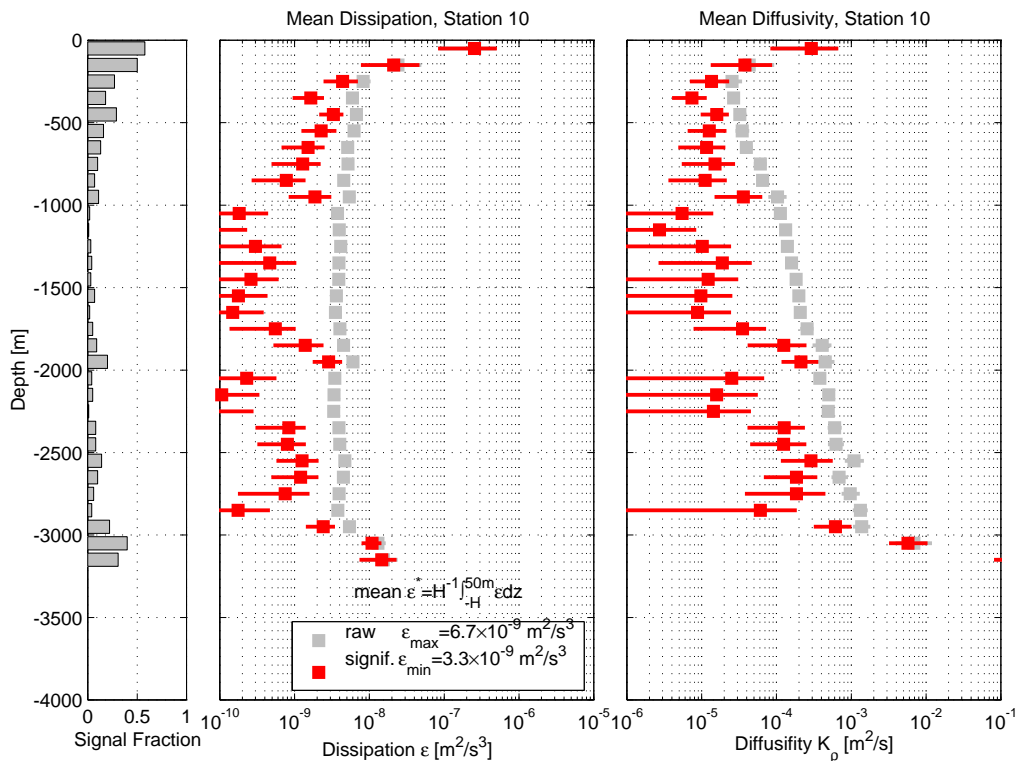


Figure 16: Dissipation and diffusivity for Station 10

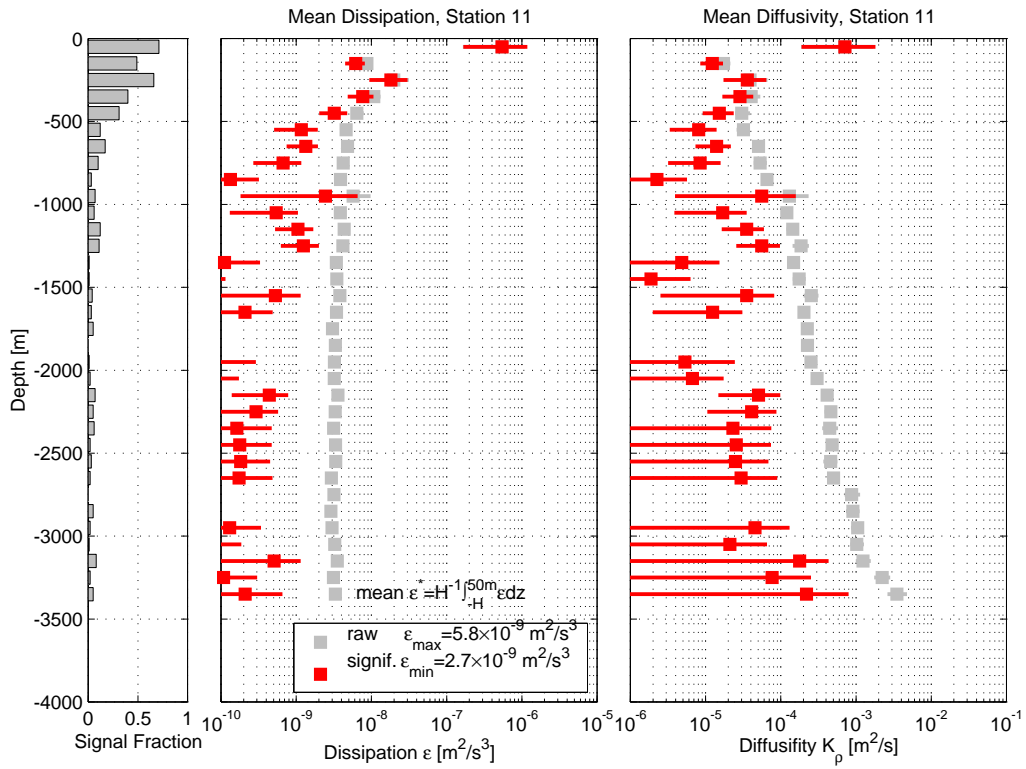


Figure 17: Dissipation and diffusivity for Station 11

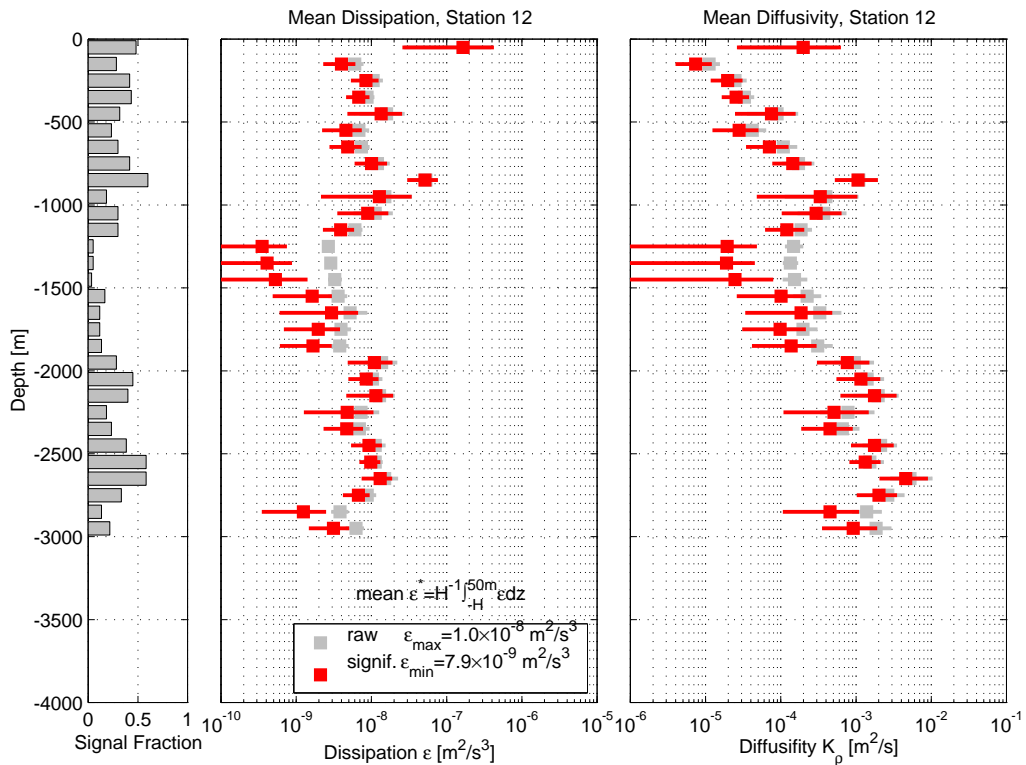


Figure 18: Dissipation and diffusivity for Station 12

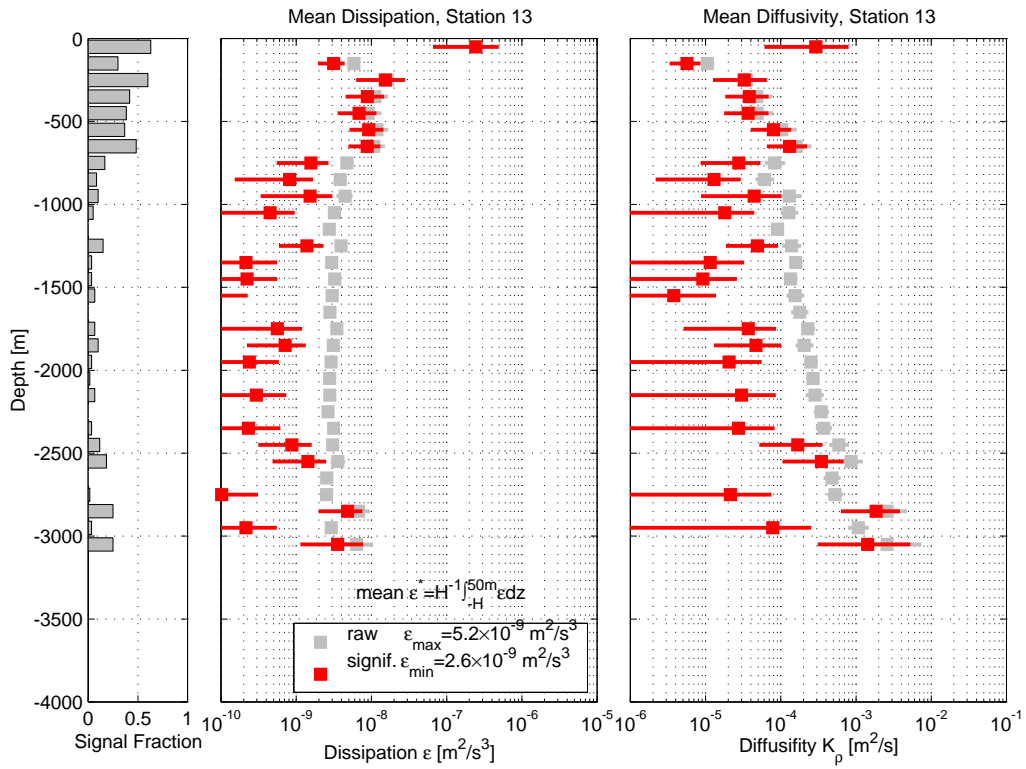


Figure 19: Dissipation and diffusivity for Station 13

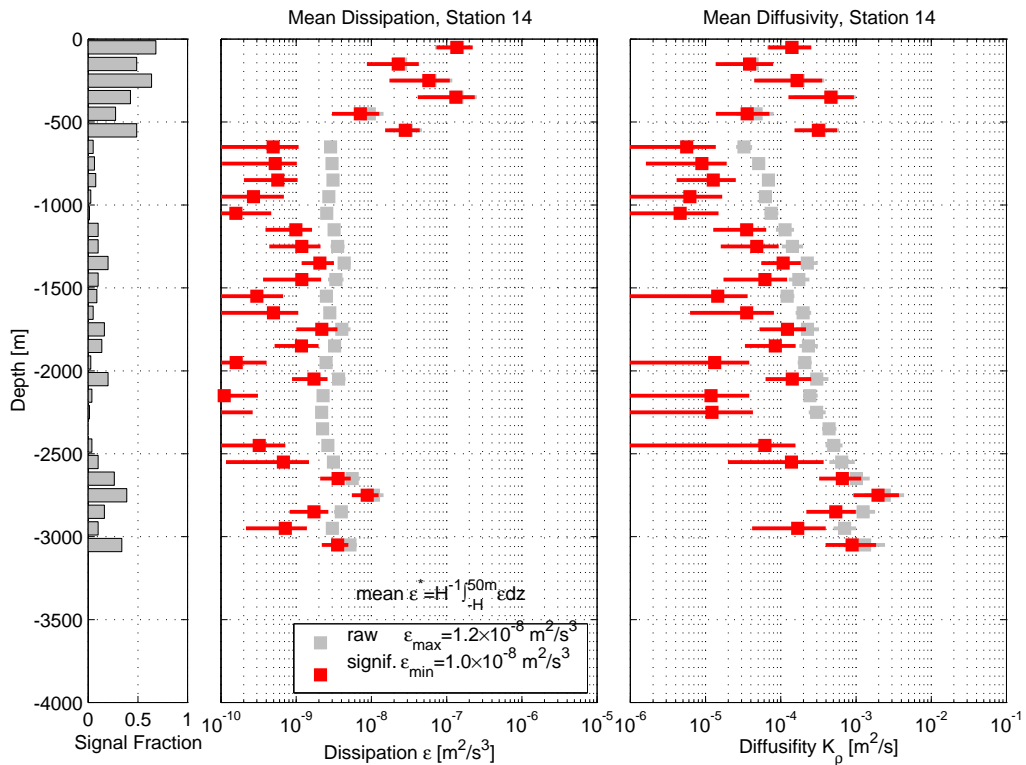


Figure 20: Dissipation and diffusivity for Station 14

data above 2000 m. Instead of changing shear probes, we altered the location of the drop weight, moving it approximately one inch off-centerline and closest to VG2. In response to this, VG1 was moved outside of the wake of the drop weight, and gave high-quality data for the final drop. Interestingly enough, VG2 also produced usable data (not ultra-low noise, but satisfactory quality) below 2000 m on the final drop. We suspect that the VG2 probe (no. 260) had a crack in it which was squeezed together under pressure, allowing it to perform properly at depth.

In the future, it might be wise to introduce an asymmetry into the fall of AVP – perhaps move the drop weights off axis without applying an unwanted torque to the instrument. In this way, the wake could be directed to one side of the instrument and the shear probes could be located on the other.

When the shear probe assemblies were removed from AVP at the end of the cruise, the whole assembly, including both shear probes and the mount for the light scattering sensor, were able to rotate around the circumference of AVP. They were not loose, but a solid bump could move them a little.

Also, each of the shear probes had gray marks on them at the end of the cruise. These came from bumping the white silicone tip with the threads of the sensor protecting shield. Evidently, the probes get hit often when removing and replacing their covers.

6.2. Appendix B: Matlab Routines for Analysis

I have written matlab routines (`calibrate_vg2` in particular) to estimate ϵ by integrating the shear spectrum and using the universal Nasmyth form for wavenumbers greater than the Kolmogorov wavenumber or 30 cpm, whichever comes first. The 30 cpm cutoff was chosen because there is a mechanical vibration of AVP near 35 Hz, and for a first cut, I have stopped integration before this wavenumber.

Programs used:

1) General Programs:

`define_stations`:

Defines the station locations, file numbers, names, indices etc for each station location.

`abstext`:

A neat little routine to put text anywhere on a matlab figure.

1) to estimate shear:

`calibrate_vg1` `calibrate_vg2`:

Produces 5 m binned dissipation data for shear probe 1 or 2 and places the data in the `diss/` directory. Requires: `nasmyth`:

the Nasmyth spectrum (from John Dunlap).

`avp_vgtrans`:

Calculates the transfer function to get the shear signal into calibrated dissipation spectrum (from John Dunlap).

`calibrate_vg_ac2`:

As `calibrate_vg2` except it does both shear and accelerometers, and it only makes a plot of a given depth range.

`calc_krho1`, `calc_krho2`:

Plots K_ρ , ϵ , N^2 and S^2 from the diss files for a single drop.

`view_diss`:

Plots the time series of shear, low-pass filtered at 20-30 Hz to remove the Seabird pump contamination and high-passed at 0.5 Hz to remove the instrument rotation rate

`plot_eps_krho_avg2`:

Plots station averaged K_ρ and dissipation from the `diss/diss` files; this also calculates the depth averaged (bootstrapped) dissipation. Station averaged dissipation (as a function of depth) and associated errors are saved into the files `/diss/avg_stat_N.mat`. Requires `estimate_shear_noise` to have been previously run on the range of files of interest.

`estimate_shear_noise`: Plots the pdf of ϵ below 500m, calculates μ and σ , and adds this information to the diss files.

`plot_station_dissipation`: Makes a nice plot of the dissipation as a function of depth for each profile in a given station.

`plot_eps_vs_flux2`:

Makes five different plots which relate the flux to the integrated dissipation. Requires that most of the programs above be run first in order to have the mean of ϵ defined at each station.

2) To estimate flux:

`calc_elflux2`:

and `calc_elflux_2000`, which does the calculations based on the upper 2000 m alone) calculates energy flux and plots a variety of aspects of the internal wave field, such as vertical displacement, KE, PE, errors, waterfall plots, hodographs, etc.

requires:

`plot_bathy`

`plot_waterfalls`

plot_vertical_dist
estimate_error
plot_ke_pe
plot_flux_map
plot_hodo
make_ascii_diss:
makes ascii files of the dissipation as a function of depth
(5 meter intervals)